P-ISSN: 2987-7261
E-ISSN: 2987-7253

Jurnal Riset Ilmu Teknik
Journal homepage: https://jurnaljepip.com/index.php/jurit
Vol 2, No. 3, pp. 189-203, 2026
DOI: doi.org/10.59976/jurit. v4i2.379

Analysis of Land-Cover Change Patterns and Their Temporal Association with Flood Occurrence in West Kendari District

Muh. Agung Apri Mars[1*], Safril Kasim[2], La Gandri[3]
Universitas Halu Oleo, Kendari, Indonesia
*Corresponding Author: aprimrss@gmail.com

ABSTRACT

Urban expansion can alter land cover and reduce the land's capacity to absorb rainfall, thereby increasing surface runoff and flood potential. West Kendari District, part of Kendari City, Southeast Sulawesi Province, experienced substantial land cover change over the past decade and suffered severe flooding in 2024. This study aimed to analyze land cover change patterns in the district between 2014 and 2024 and to describe the temporal relationship between these changes and reported flood occurrences, without quantifying economic losses. Land cover was classified from Landsat 8 OLI/TIRS imagery for 2014 and 2019 and Landsat 9 OLI2/TIRS2 imagery for 2024, all at 30 meter spatial resolution and obtained from the USGS EarthExplorer archive, using the Maximum Likelihood Classification method into six classes. Classification accuracy was evaluated through a confusion matrix, with field validation using 26 reference points available only for the 2024 map, yielding an overall accuracy of 88.46 percent and a corrected Kappa coefficient of 0.851, indicating almost perfect agreement. The spatial analysis showed that forest cover declined by 412.47 hectares (36.8 percent), settlement area increased by 235.91 hectares (52.1 percent), and shrubland expanded by 362.51 hectares (502.6 percent), with the dominant transitions occurring from forest to shrubland and mixed garden, and from mixed garden to settlement. Flood events recorded by the Kendari City Regional Disaster Management Agency rose from none in 2014 to three in 2019 and five in 2024, coinciding in time with forest loss and settlement expansion, although a causal relationship could not be confirmed due to other contributing factors such as rainfall, drainage capacity, river conditions, sedimentation, and tidal influence. Further research incorporating rainfall data and economic loss assessment is recommended.

Keywords: *Land-Cover Change, Maximum Likelihood Classification, Accuracy Assessment, Flood Occurrence.*

Manuscript received 09 July. 2026; revised 24 August. 2026; accepted 30 August. 2026.

INTRODUCTION

Climate change is a major global environmental issue that has increased the frequency and intensity of hydrometeorological disasters, including floods. More frequent extreme rainfall in many regions is placing growing pressure on natural hydrological systems, resulting in floods that occur more often and affect larger numbers of people [1]. In Indonesia, floods have remained the country's most prevalent disaster over the past decade, causing substantial damage to the environment and infrastructure and disrupting communities' social and economic activities [2], [3].

The rise in flood occurrence is driven not only by climatic factors but also by land-cover change. Converting forests and other vegetated land into settlements and built-up areas reduces the soil's capacity to absorb rainfall and increases the extent of impervious surfaces. As a result, surface runoff rises, making it more likely that rivers and drainage systems will exceed their capacity during high-intensity rainfall [4],[5], [6], [7]. Land-cover change is therefore an important factor that heightens an area's vulnerability to flooding.

Kendari is one of Indonesia's rapidly developing cities, and this growth has placed increasing pressure on land use. [8], [9] found that more than half of the city may be exposed to flooding, while [10], [11] reported that both the extent of inundation and the frequency of floods had increased over the preceding decade. The expansion of settlements and infrastructure without corresponding improvements in sustainable spatial planning has reduced water-catchment areas and increased the risk of urban flooding [12], [13].

One area under particular pressure from land-cover change is Nipa-Nipa Grand Forest Park, which serves as a catchment area for Kendari City. The conversion of forest into cultivated and built-up land has weakened the area's ecological role in regulating surface runoff and maintaining the local water balance [14], [15]. This decline in the environmental quality of Nipa-Nipa Grand Forest Park has contributed to greater flood potential in downstream areas, including West Kendari District [16], [17].

West Kendari District was among the areas most severely affected by the 2024 flood. According to the Kendari City Regional Disaster Management Agency [18], at least 561 houses were affected, and public facilities in Sodohoa Urban Village, including a school and a hospital, were damaged. In addition to the physical damage, residents suffered considerable economic losses from damage to their homes, furniture, electronic equipment, and other household assets [19], [20].

Despite the scale of these flood impacts, previous studies in Kendari have generally treated flood-prone-area mapping [21], [22] and land-cover dynamics [23], [24] as separate topics, and none has combined an area-consistent, multi-temporal land-cover account with a documented flood-event record specifically for West Kendari District. This leaves two questions that the available data can address: (1) how has land cover in West Kendari District changed between 2014 and 2024, and which transition pathways dominate that change; and (2) does the temporal pattern of reported flood occurrence in the district coincide with these land-cover changes. As explained further below, the available data can describe this temporal coincidence but cannot support a statistical test of causation between the two.

The three observation years, 2014, 2019, and 2024, were selected to provide two five-year change intervals bracketing the major flood event of 2024 discussed above, consistent with the availability of cloud-screened Landsat scenes over the district. Because the Landsat scenes used for the three years were not necessarily acquired in the same month, they could not be matched precisely for season, tidal stage, or antecedent rainfall condition; this limits the comparability of the coastal classes (water body and mangrove) in particular and is discussed further in the Study Limitations subsection.

Hydrologically, West Kendari District lies within a coastal catchment that drains toward Kendari Bay and is crossed by several small rivers, including the Watu-Watu, Tipulu, and Lahundape rivers, whose watersheds do not follow the district's administrative boundary. Because rainfall-runoff processes are governed by watershed rather than administrative limits, land-cover change both inside and immediately upstream of the district, including within the adjoining Nipa-Nipa catchment, is potentially relevant to flood generation in West Kendari District. The present study nevertheless quantifies land-cover change only within the administrative boundary of the district, which is used here as an approximation of the area contributing runoff to the district and is noted as a limitation of the spatial scope of the analysis.

Flood occurrence in a coastal urban district such as West Kendari is influenced by multiple, interacting factors in addition to land cover. Rainfall intensity and duration determine the volume of water entering the drainage system; topography and soil characteristics influence infiltration and the speed of runoff concentration; the capacity and physical condition of rivers and drainage channels determine how much flow can be conveyed without overtopping; sedimentation reduces channel capacity over time; and, in a coastal setting, high tides can reduce the hydraulic gradient available for drainage and cause water to back up in low-lying areas. Land-cover change interacts with these factors primarily by altering infiltration and surface roughness: converting forest and shrubland to impervious settlement is expected to increase the proportion of rainfall that becomes surface runoff and to shorten the time to peak flow. This study examines flood occurrence and frequency, that is, whether and how often flood events were reported, rather than flood extent, depth, damage, or risk, which would require hydrological or damage data that were not available for this study.

Based on this framework, the study examines the descriptive expectation that periods of greater forest loss and settlement expansion in West Kendari District coincide with a higher number of reported flood events. Observing such a temporal coincidence, however, would not by itself establish that land-cover change caused the floods, because rainfall, drainage, river capacity, sedimentation, and tides were not held constant or statistically controlled in this study; the evidence that would be needed to isolate the independent contribution of land-cover change, such as a rainfall-adjusted statistical or hydrological model, is identified in the Study Limitations subsection.

Building on this gap, this study aims to (1) analyze land-cover change patterns in West Kendari District between 2014 and 2024 using a reconciled, area-consistent classification, and (2) describe the temporal association between these changes and reported flood occurrence in the district. Economic-loss quantification, although relevant to the impacts described above, requires valuation data that were not collected for this study and is therefore not among its objectives; it is recommended as a direction for future research. The findings are intended to inform, rather than conclusively determine, spatial planning, water-catchment management, and flood-mitigation strategies in West

Kendari District.

METHODS

Land cover was analyzed through supervised classification using the Maximum Likelihood Classification (MLC) algorithm. This method was selected because it assigns pixels to classes on the basis of statistical probability and can therefore produce highly accurate classifications when training data are representative. The analysis involved image preprocessing, image-data processing, accuracy assessment, and spatial (overlay) analysis to identify land-cover change in 2014, 2019, and 2024, followed by a descriptive comparison with the district's flood-event record.

Figure 1 summarizes the overall workflow, from image acquisition through classification, validation, change detection, and flood-data comparison.

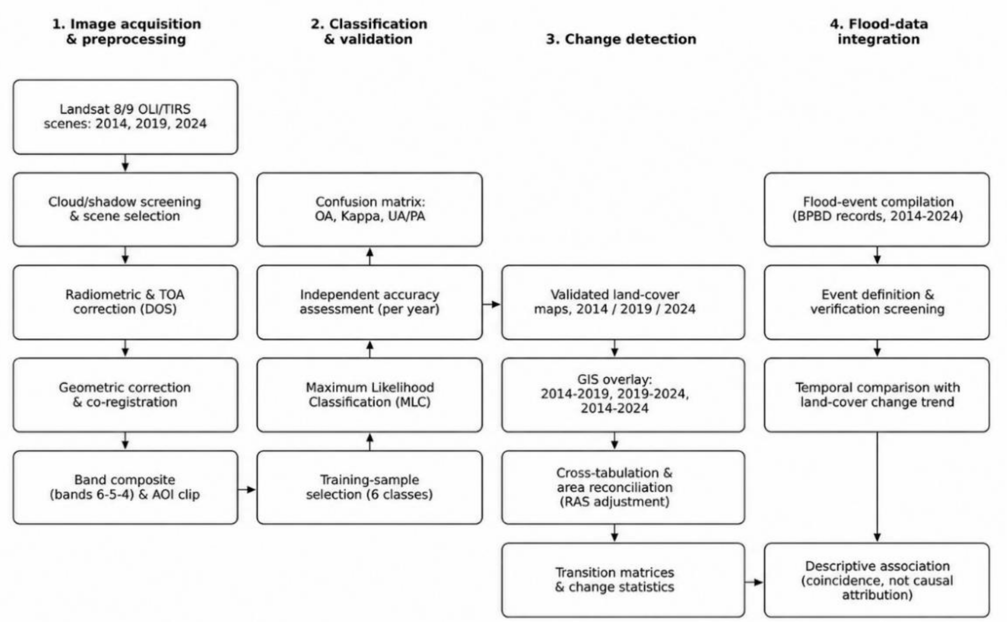

Figure 1. Workflow of image acquisition, preprocessing, classification, validation, change detection, and flood-data comparison

Study Area

West Kendari District is one of eleven administrative districts of Kendari City, the capital of Southeast Sulawesi Province, Indonesia. Kendari City occupies the southeastern peninsula of Sulawesi and surrounds Kendari Bay, lying at approximately 3°54′–4°3′ South latitude and 122°26′–122°39′ East longitude, on hilly coastal terrain. Based on the classified Landsat imagery used in this study, West Kendari District covers approximately 2,247.74 ha (22.48 km^2).

The district borders Kendari Bay to the south and east, so its coastal fringe, including the water-body and mangrove classes, is additionally influenced by tides. The northern part of the district is hilly and forested and forms part of the water-catchment area that feeds the district's rivers, while the flatter southern part along the coastline is more densely settled. Several small rivers, including the Watu-Watu, Tipulu, and Lahundape rivers, drain the district toward Kendari Bay. The district has a tropical climate with wet and dry seasons influenced by the Asian and Australian monsoons and, like the rest of Kendari City, has experienced rapid population growth and settlement expansion over the past decade. All spatial data in this study were processed in the WGS 1984 datum, UTM Zone 51S projection, consistent with the coordinate system shown in Figure 2.

Satellite Image Data

Table 1 lists the satellite image data used to classify land cover in 2014, 2019, and 2024. All scenes were obtained from the United States Geological Survey (USGS) EarthExplorer archive at 30 m spatial resolution for the multispectral bands used in classification. Fields that depend on the specific scene identifiers used by the authors are marked for confirmation.

Image Preprocessing

Image preprocessing was conducted to improve image quality before classification. The first step was geometric correction, which rectified geometric distortion so that the location of objects in the images corresponded to their actual positions on the ground (Wulansari, 2017). Co-registration among the 2014, 2019, and 2024 scenes was checked against stable ground features to keep the relative positional error within approximately one 30 m pixel, reducing the chance that misalignment between scenes would be mistaken for genuine land-cover change.

Atmospheric correction followed a fixed sequence, applied identically to every scene to support comparability across sensors and years. First, raw digital numbers were converted to Top-of-Atmosphere (TOA) reflectance using the scene-specific rescaling coefficients provided in each image's metadata file. Second, the atmospheric path radiance in each band was estimated using the Dark Object Subtraction (DOS) method, which assumes that the darkest pixels in a scene, such as deep water or cloud shadow, should have a surface reflectance near zero; any positive digital number recorded for these pixels is therefore attributed to atmospheric scattering and subtracted from the entire band. Third, the DOS-corrected values were treated as an approximation of surface reflectance for classification. This TOA-then-DOS sequence was applied to both the Landsat 8 OLI/TIRS scenes (2014 and 2019) and the Landsat 9 OLI-2/TIRS-2 scene (2024); because Landsat 8 and Landsat 9 were not independently cross-calibrated in this study, small residual differences in reflectance between the two sensors cannot be ruled out and are noted as a limitation. Cloud and cloud-shadow pixels were identified and masked using the quality-assessment band supplied with each Landsat product prior to classification.

Next, layer stacking was used to combine several bands into a vegetation-analysis composite comprising bands 6, 5, and 4. Because West Kendari District is covered by a single Landsat scene, mosaicking of multiple scenes was not required. Finally, the images were cropped to the Area of Interest (AOI) in Geographic Information System (GIS) software, ensuring that the analysis covered only the study area [25], [26].

Image-Data Processing

Six land-cover classes were defined a priori on the basis of dominant vegetation structure and land use: water body, mangrove, settlement, forest, mixed garden, and shrubland. Mixed garden was defined as land under a combination of tree crops and seasonal crops, distinguished from closed-canopy forest and from shrubland, which was defined as land dominated by sparse woody or secondary vegetation. Image-data processing involved selecting training samples and classifying land cover [18], [27], [28]. Training-sample selection is critical because classification quality depends strongly on how well the samples represent each land-cover class. Training samples for each year were selected independently by visual interpretation of the corresponding false-color composite, supported by familiarity with the study. The Maximum Likelihood Classification (MLC) algorithm was then used to assign every pixel to the class for which it had the highest posterior probability [29], [30].

The MLC decision rule used in this study is:

$$P(i|X) = \frac{P(X|i) \times P(i)}{P(X)} \tag{1}$$

where $P(i|X)$ is the posterior probability that pixel X belongs to class i; $P(X|i)$ is the likelihood of observing spectral vector X given class i, modeled as a multivariate normal distribution in standard MLC implementations; $P(i)$ is the prior probability of class i (assumed equal across classes unless stated otherwise); and $P(X)$ is the overall (marginal) probability of observing X, which acts as a normalizing constant and is identical for all classes being compared for a given pixel. Each pixel X is assigned to the class i that maximizes $P(i|X)$.

Accuracy Assessment

Classification accuracy was evaluated using a confusion matrix, which cross-tabulates the classified land-cover map against independent reference data collected in the field and thereby indicates the reliability of the classification [31], [32]. Independent field reference data of this kind were collected only for the 2024 classification, using 26 sample points distributed across the six land-cover classes; the samples used for accuracy assessment were independent of those used to train the classifier. The 2014 and 2019 classifications were not accompanied by a contemporaneous, independent field validation, so no confusion matrix is reported for those two years; their accuracy is therefore unknown and the maps should be treated as descriptive rather than field-verified. This limitation is discussed further below and in Study Limitations.

From the confusion matrix, two related but distinct statistics were calculated: overall accuracy and the Kappa coefficientt [33], [34]. Overall accuracy is the proportion of reference points correctly classified, $OA = \Sigma X_{ii} / N$, where X_{ii} is the number of correctly classified reference points in class i (the diagonal of the confusion matrix) and N is the total number of reference points. The Kappa coefficient additionally corrects for the agreement expected by chance and is calculated as:

$$K = \frac{N \times \sum X_{ii} - \sum (X_{i+} \times X_{+i})}{N^2 - \sum (X_{i+} \times X_{+i})} \tag{2}$$

where K is the Kappa coefficient; X_{ii} is the diagonal value of the confusion matrix in row i and column i (the number of correctly classified reference points for class i); X_{i+} is the row total for class i (the total number of points classified as class i); X_{+i} is the column total for class i (the total number of reference points actually belonging to class i); N is the total number of sample points (N = 26); and r is the number of land-cover classes (r = 6). Overall accuracy and

Kappa are reported separately in the Results section because they measure related but different quantities: overall accuracy is a simple percentage of correct classifications, whereas Kappa expresses agreement after removing the portion attributable to chance and is interpreted using the scale in Table 2 rather than read as a percentage.

Table 2. Interpretation of Kappa Coefficient Values

Kappa Value	Level of Agreement
< 0.00	Less than chance agreement
0.01–0.20	Slight agreement
0.21–0.40	Fair agreement
0.41–0.60	Moderate agreement
0.61–0.80	Substantial agreement
0.81–0.99	Almost perfect agreement

Flood-Event Data

Flood-event information for 2014, 2019, and 2024 was compiled from situation reports of the Kendari City Regional Disaster Management Agency (BPBD Kendari City, A flood event was defined as a single reported occurrence of inundation affecting residential areas of West Kendari District on a given date, regardless of its areal extent or duration; multiple inundation reports on the same date and in the same general location were treated as one event. Where possible, each candidate event was cross-checked against at least one additional independent source, such as local news reporting; events reported in only a single, unverified source were excluded. A recorded count of zero flood events in 2014 indicates the absence of a BPBD-verified event on record for that year, not confirmed field evidence that no inundation occurred, because routine hydrometeorological monitoring and community reporting were less systematic in 2014 than in later years. This asymmetry in reporting effort over time is treated as a limitation when interpreting the flood-event trend, since it can inflate the apparent increase in flood frequency independently of any change in the underlying flood-generating processes. Table 8 (Results) lists the available flood events with date, approximate location, source, and available impact information; corresponding rainfall records and precise geographic coordinates for each event were not available to the authors at the time of writing and are recommended for future work.

Spatial Overlay Analysis

Land-cover change was analyzed using an overlay technique, in which land-cover maps from different years are superimposed to reveal spatial changes between periods. The 2014 map was overlaid with the 2019 map, the 2019 map with the 2024 map, and the 2014 map with the 2024 map. These overlays were used to calculate changes in the area of each land-cover class and identify the patterns that occurred during the study period (Sejati et al., 2024). Cross-tabulation in Microsoft Excel was then used to quantify transitions between land-cover classes.

Because the class areas produced independently for each year did not sum to an identical total district area (raw totals of 2,247.74 ha, 2,245.01 ha, and 2,243.95 ha for 2014, 2019, and 2024, respectively, against an expected constant boundary area), the class areas reported in Table 3 and the transition areas reported in Tables 5, 6, and 7 were reconciled to a common total of 2,247.74 ha using iterative proportional fitting (the RAS algorithm). This procedure rescales matrix cells to satisfy independently known row and column totals while preserving, as closely as possible, the relative pattern of the original cross-tabulation; it corrects small rounding and raster-to-vector conversion discrepancies and does not alter the dominant transition pathways identified in the original overlay. Reconciled transition values below approximately 0.5 ha, corresponding to fewer than about five 30 m Landsat pixels, are retained in the tables for completeness but should be interpreted with caution, since at this resolution they may reflect mixed pixels, small co-registration offsets, residual classification error, or short-term tidal variation rather than a confirmed land-cover conversion.

Finally, the reconciled land-cover results were compared with the flood-event record described above as a descriptive, temporal comparison; this comparison does not constitute a statistical, spatial, or hydrological test of a relationship between land-cover change and flood occurrence, for the reasons discussed in the Introduction and Study Limitations.

RESULTS AND DISCUSSION

Land Cover in West Kendari District

Land cover in West Kendari District was mapped from processed satellite imagery for 2014, 2019, and 2024. The digitized data provided the basis for assessing land-cover change over the ten-year period from 2014 to 2024. The maps distinguish six land-cover classes, each shown in a different color. Forest, shown in dark green, dominates the northern part of the district. Mixed garden, shown in yellow, is generally located in the transition zone between forest and settlements. Settlements, shown in gray, are widely distributed across the southern part of the district, particularly along the coastline. Shrubland, shown in pink, occurs around mixed gardens and settlements. Mangroves, shown in brown, are present along the southwestern coast, while water bodies such as Kendari Bay are shown in light blue. Figure 2 presents the land-cover maps.

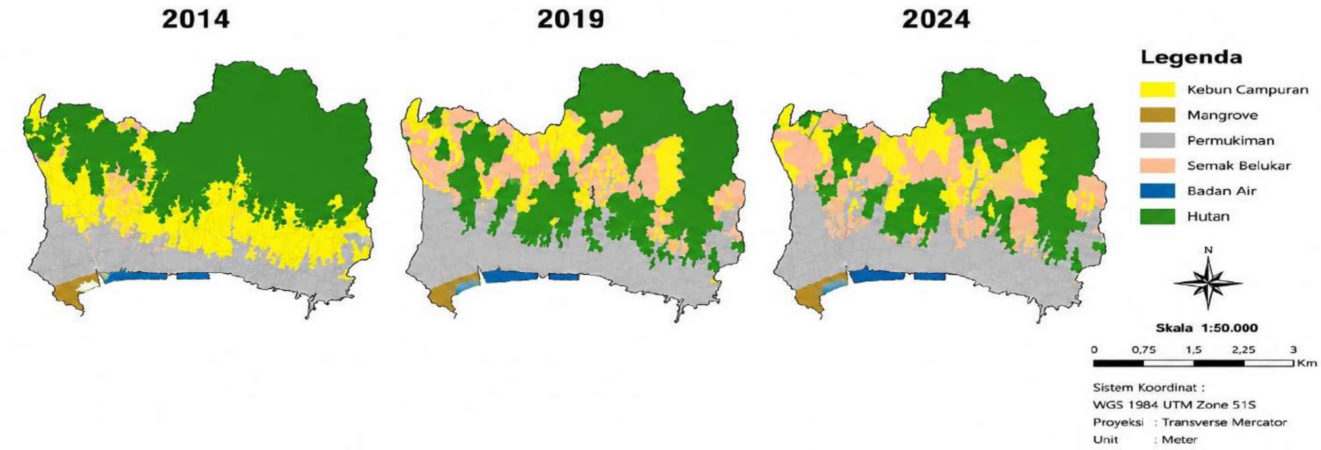

Figure 2. Land-Cover Maps of West Kendari District, 2014, 2019, and 2024

The area figures below have been recalculated so that the class areas for each year sum exactly to the district's boundary area of 2,247.74 ha, correcting small rounding and raster-to-vector discrepancies present in the original tabulation; the corrected figures differ from the originally reported values by at most about 0.2% and do not change the overall pattern of change. Table 3 presents the corrected area of each land-cover class.

Table 3. Land Cover in West Kendari District in 2014, 2019, and 2024

No.	Land-Cover Class	2014 (ha)	2014 (%)	2019 (ha)	2019 (%)	2024 (ha)	2024 (%)
1	Water Body	27.07	1.2	30.21	1.3	29.77	1.3
2	Forest	1119.92	49.8	891.06	39.6	707.45	31.5
3	Mixed Garden	561.62	25.0	275.13	12.2	375.12	16.7
4	Mangrove	14.09	0.6	10.74	0.5	11.94	0.5
5	Settlement	452.91	20.1	648.43	28.8	688.82	30.6
6	Shrubland	72.13	3.2	392.17	17.4	434.64	19.3
	Total	2,247.74	100.0	2,247.74	100.0	2,247.74	100.0

As shown in Table 3, forest was the largest land-cover class in West Kendari District in 2014, covering 1,119.92 ha (49.8%), followed by mixed garden at 561.62 ha (25.0%), settlement at 452.91 ha (20.1%), shrubland at 72.13 ha (3.2%), water bodies at 27.07 ha (1.2%), and mangroves at 14.09 ha (0.6%). By 2019, forest covered 891.06 ha (39.6%), settlement 648.43 ha (28.8%), shrubland 392.17 ha (17.4%), mixed garden 275.13 ha (12.2%), water bodies 30.21 ha (1.3%), and mangroves 10.74 ha (0.5%). By 2024, forest had declined to 707.45 ha (31.5%), while settlement covered 688.82 ha (30.6%), shrubland 434.64 ha (19.3%), mixed garden 375.12 ha (16.7%), water bodies 29.77 ha (1.3%), and mangroves 11.94 ha (0.5%).

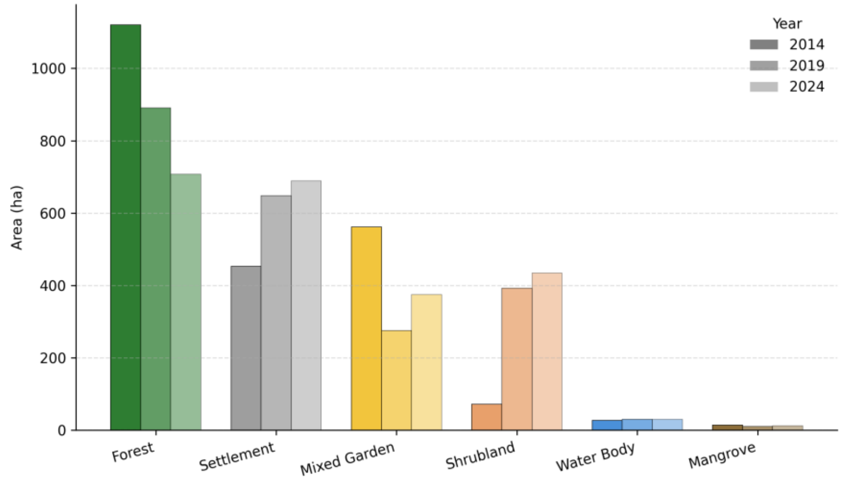

Figure 3. Land Cover in West Kendari District

Accuracy Assessment of the Land-Cover Classification

Classification accuracy was assessed by comparing the digitally classified land-cover map with test samples collected during fieldwork. The samples used as training areas were different from those used for the accuracy assessment, which were collected at separate locations to provide an independent evaluation. This assessment applies to the 2024 classification only, using 26 sample points across the six land-cover classes; corresponding independent reference data were not available for 2014 or 2019, so no accuracy statistics are reported for those years. Table 4 presents the confusion matrix for the 2024 map, together with class-level user's and producer's accuracy.

Table 4. Confusion Matrix and Class-Level Accuracy for the 2024 Land-Cover Classification (n = 26)

Classified\Reference	Water Body	Mangrove	Settlement	Forest	Mixed Garden	Shrubland	Row Total	User's Acc.
Water Body	1	–	–	–	–	–	1	100.0%
Mangrove	–	1	–	–	–	–	1	100.0%
Settlement	–	–	6	–	1	–	7	85.7%
Forest	–	–	–	7	1	–	8	87.5%
Mixed Garden	–	–	–	1	3	–	4	75.0%
Shrubland	–	–	–	–	–	5	5	100.0%
Column Total	1	1	6	8	5	5	26	
Producer's Accuracy	100.0%	100.0%	100.0%	87.5%	60.0%	100.0%		

Overall accuracy, defined as the proportion of reference points correctly classified, was ΣXii/N = 23/26 = 88.46%. Using the Kappa formula defined in Methods, the sum of the diagonal (ΣXii) is 23, and the sum of the row-total-by-column-total cross-products (ΣXi+ × X+i) is (1×1) + (1×1) + (7×6) + (8×8) + (4×5) + (5×5) = 1 + 1 + 42 + 64 + 20 + 25 = 153. The corrected Kappa coefficient is therefore:

$$K = (26 \times 23 - 153) / (26^2 - 153) = (598 - 153) / (676 - 153) = 445 / 523 = 0.8509$$

that is, K ≈ 0.851. Because the expected-agreement cross-product sum in the original submission was calculated as 154 rather than 153, the previously reported Kappa of 0.8503 is superseded by this corrected value of 0.8509; the difference is small and does not change the qualitative conclusion. Overall accuracy (88.46%) and Kappa (0.851) are reported separately because they answer different questions: overall accuracy is the simple percentage of correctly classified reference points, while Kappa additionally discounts the agreement that would be expected by chance given the observed row and column totals. Given the small reference sample (N = 26), an approximate 95% confidence interval for overall accuracy, based on a normal approximation to the binomial distribution, is wide (about 76% to 100%); this wide interval reflects the small sample size and should be considered when judging the precision of the reported accuracy, particularly for the water-body and mangrove classes, which were each represented by only a single reference point (Table 4). According to Viera and Garrett (2005), as cited in Muhammad et al. (2016), a Kappa value above 0.81 falls within the 'almost perfect' category. Class-level user's accuracy ranged from 75.0% (mixed garden) to 100% (water body, mangrove, and shrubland), and producer's accuracy ranged from 60.0% (mixed garden) to 100% (water body, mangrove, settlement, and shrubland), indicating that confusion, where it occurred, was concentrated around the mixed-garden class (Table 4). Because independent validation of this kind is available only for 2024, this accuracy assessment supports the 2024 land-cover map specifically; it does not establish, and should not be generalized to, the accuracy of the 2014 or 2019 classifications.

Dynamics of Land-Cover Change in West Kendari District

Land-cover dynamics were examined by overlaying the 2014 and 2019 maps, the 2019 and 2024 maps, and the 2014 and 2024 maps. The results reveal how the area of each land-cover class changed into other classes. Nineteen types of transition were identified and grouped according to six original land-cover classes:

- Forest changed to mixed garden, settlement, or shrubland, or remained forest.
- Settlement changed to shrubland or remained settlement.
- Water body changed to settlement or mangrove, or remained water body.
- Mangrove changed to settlement or water body, or remained mangrove.
- Shrubland changed to settlement or mixed garden, or remained shrubland.
- Mixed garden changed to settlement, shrubland, or forest, or remained mixed garden.

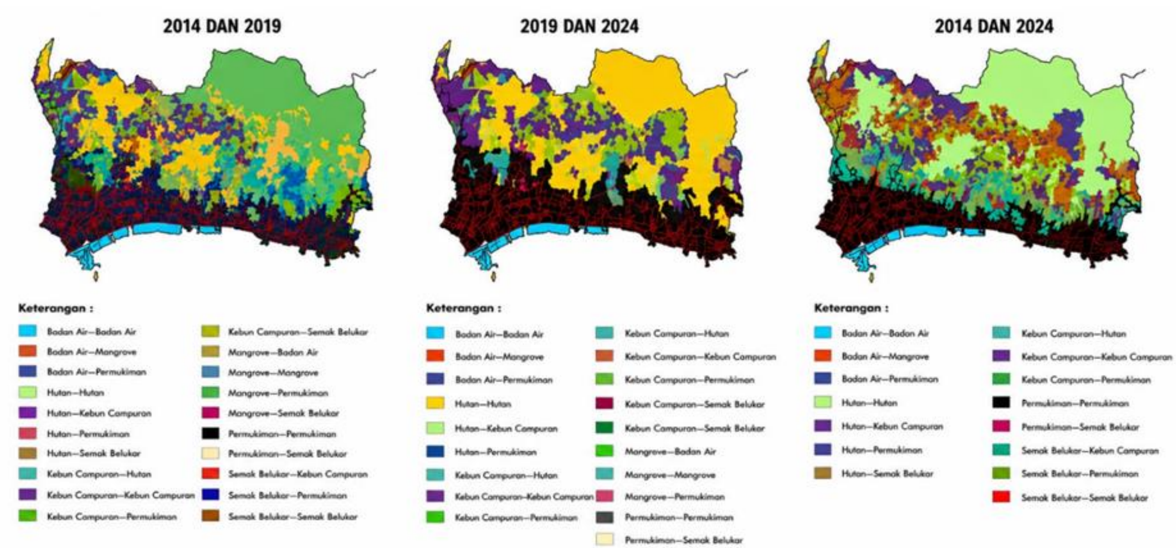

Figure 4. Overlay Maps of Land-Cover Change, 2014–2019, 2019–2024, and 2014–2024

Figure 5 presents the land-cover change maps produced by overlaying the data for 2014–2019, 2019–2024, and 2014–2024. The corresponding transition areas, reconciled so that the row and column totals of each table match the corrected figures in Table 3 (see Methods, Spatial Overlay Analysis), are presented in Tables 5, 6, and 7.

Table 5. Corrected Land-Cover Change Dynamics in West Kendari District, 2014–2019

No.	Class, start year	Class, end year	Area (ha)	Status
1	Water Body	Water Body	26.85	Unchanged
2	Water Body	Mangrove	0.13	Changed
3	Water Body	Settlement	0.09	Changed
4	Mangrove	Water Body	3.30	Changed
5	Mangrove	Mangrove	10.58	Unchanged
6	Mangrove	Settlement	0.21	Changed
7	Settlement	Settlement	450.04	Unchanged
8	Settlement	Shrubland	2.87	Changed
9	Forest	Settlement	12.74	Changed
10	Forest	Forest	662.72	Unchanged
11	Forest	Mixed Garden	180.90	Changed
12	Forest	Shrubland	263.56	Changed

No.	Class, start year	Class, end year	Area (ha)	Status
13	Shrubland	Settlement	41.58	Changed
14	Shrubland	Mixed Garden	15.14	Changed
15	Shrubland	Shrubland	15.41	Unchanged
16	Mixed Garden	Settlement	143.78	Changed
17	Mixed Garden	Forest	228.41	Changed
18	Mixed Garden	Mixed Garden	79.09	Unchanged
19	Mixed Garden	Shrubland	110.34	Changed

Table 5 summarizes reconciled land-cover transitions in West Kendari District between 2014 and 2019. Most classes were dominated by persistence: 450.04 ha of settlement, 662.72 ha of forest, and 26.85 ha of water body remained in the same class. Forest also changed substantially, with 180.90 ha converting to mixed garden, 263.56 ha to shrubland, and 12.74 ha to settlement. Mixed garden changed into several other types, including 228.41 ha to forest, 143.78 ha to settlement, and 110.34 ha to shrubland, while 79.09 ha remained mixed garden. Shrubland changed to settlement (41.58 ha) and mixed garden (15.14 ha), while 15.41 ha remained shrubland. Small coastal transitions, such as water body to mangrove (0.13 ha) and mangrove to settlement (0.21 ha), are retained for completeness but, at 30 m resolution, correspond to only a few pixels and should be interpreted with caution rather than as confirmed conversions.

Table 6. Corrected Land-Cover Change Dynamics in West Kendari District, 2019–2024

No.	Class, start year	Class, end year	Area (ha)	Status
1	Water Body	Water Body	29.02	Unchanged
2	Water Body	Mangrove	1.18	Changed
3	Water Body	Settlement	0.01	Changed
4	Mangrove	Water Body	0.18	Changed
5	Mangrove	Mangrove	10.55	Unchanged
6	Mangrove	Settlement	0.01	Changed
7	Settlement	Settlement	639.57	Unchanged
8	Settlement	Shrubland	8.86	Changed
9	Forest	Settlement	36.91	Changed
10	Forest	Forest	693.24	Unchanged
11	Forest	Mixed Garden	50.36	Changed
12	Forest	Shrubland	110.55	Changed
13	Shrubland	Settlement	5.49	Changed
14	Shrubland	Mixed Garden	82.86	Changed
15	Shrubland	Shrubland	303.82	Unchanged
16	Mixed Garden	Settlement	7.06	Changed
17	Mixed Garden	Forest	14.51	Changed
18	Mixed Garden	Mixed Garden	242.00	Unchanged
19	Mixed Garden	Shrubland	11.56	Changed

Table 6 presents reconciled land-cover transitions between 2019 and 2024. Settlement (639.57 ha), forest (693.24 ha), and shrubland (303.82 ha) again showed the largest persistent areas. Forest lost 110.55 ha to shrubland, 50.36 ha to mixed garden, and 36.91 ha to settlement. Mixed garden gained 82.86 ha from shrubland and lost 11.56 ha to shrubland, 7.06 ha to settlement, and 14.51 ha to forest, while 242.00 ha remained mixed garden. Coastal transitions, including water body to mangrove (1.18 ha) and mangrove to water body (0.18 ha), remained small relative to the interior transitions and, as above, should be interpreted cautiously given the spatial resolution of the imagery.

Table 7. Corrected Land-Cover Change Dynamics in West Kendari District, 2014–2024

No.	Class, start year	Class, end year	Area (ha)	Status
1	Water Body	Water Body	26.79	Unchanged
2	Water Body	Mangrove	0.26	Changed
3	Water Body	Settlement	0.02	Changed
4	Mangrove	Water Body	2.60	Changed
5	Mangrove	Mangrove	11.47	Unchanged
6	Mangrove	Settlement	0.02	Changed
7	Settlement	Settlement	441.74	Unchanged
8	Settlement	Shrubland	11.17	Changed
9	Forest	Settlement	6.91	Changed
10	Forest	Forest	574.10	Unchanged
11	Forest	Mixed Garden	248.30	Changed
12	Forest	Shrubland	290.61	Changed
13	Shrubland	Settlement	49.38	Changed
14	Shrubland	Mixed Garden	17.03	Changed
15	Shrubland	Shrubland	5.72	Unchanged
16	Mixed Garden	Settlement	191.05	Changed
17	Mixed Garden	Forest	133.64	Changed
18	Mixed Garden	Mixed Garden	109.79	Unchanged
19	Mixed Garden	Shrubland	127.14	Changed

Table 7 shows that land-cover dynamics in West Kendari District from 2014 to 2024 were dominated by changes in forest and mixed garden. Forest was converted to shrubland over 290.61 ha, to mixed garden over 248.30 ha, and to settlement over 6.91 ha, while 574.10 ha remained forest. Mixed garden lost 191.05 ha to settlement, 127.14 ha to shrubland, and 133.64 ha to forest, while 109.79 ha remained mixed garden. Shrubland changed to settlement over 49.38 ha and to mixed garden over 17.03 ha. In the coastal zone, 0.02 ha of water body changed to settlement and 0.26 ha to mangrove, while 2.60 ha of mangrove changed to water body and 0.02 ha to settlement; consistent with the caution noted above, these coastal values are small relative to the classification's spatial resolution.

Overall, land-cover change in West Kendari District from 2014 to 2024 was dominated by the conversion of forest into shrubland and mixed garden and by the expansion of settlement. In absolute and relative terms, forest declined by 412.47 ha (–36.8%), mixed garden declined by 186.50 ha (–33.2%), settlement increased by 235.91 ha (+52.1%), shrubland increased by 362.51 ha (+502.6%), water body increased by 2.70 ha (+10.0%), and mangrove declined by 2.15 ha (–15.3%). These changes point to growing pressure on forested areas from human activity and shifts in land use, and may alter the district's hydrological characteristics by reducing the amount of rainfall that can infiltrate the soil and increasing surface runoff.

Classification Uncertainty

Because the accuracy assessment reported above applies only to the 2024 classification, the transition pathways described in Tables 5–7 for periods involving 2014 and 2019 should be interpreted as indicative rather than field-verified. The classes most likely to be confused with one another are forest, shrubland, and mixed garden, because their spectral signatures can overlap where forest is degraded, where mixed gardens carry a dense tree-crop canopy, or where shrubland is transitional secondary vegetation; the 2024 confusion matrix itself shows the lowest producer's accuracy for mixed garden (60.0%), consistent with this expected overlap. Settlement can also be confused with bare or newly cleared land during active land conversion. This spectral overlap means that some of the reported forest-to-shrubland and forest-to-mixed-garden transitions may partly reflect classification uncertainty rather than confirmed land-cover conversion, particularly near class boundaries.

Reported Flood Occurrence in West Kendari District

Table 8 lists the flood events available in BPBD records for West Kendari District. Detailed event-level information (exact date, rainfall, and precise location) was available primarily for the major 2024 event; the remaining events are reported at the level of detail available in the source records, and the gaps are noted explicitly rather than filled with unverified figures.

Figure 7 presents forest area, settlement area, and the number of reported flood events over the three observation years side by side, purely as a descriptive visualization; it is not a statistical test and should not be read as demonstrating a causal relationship.

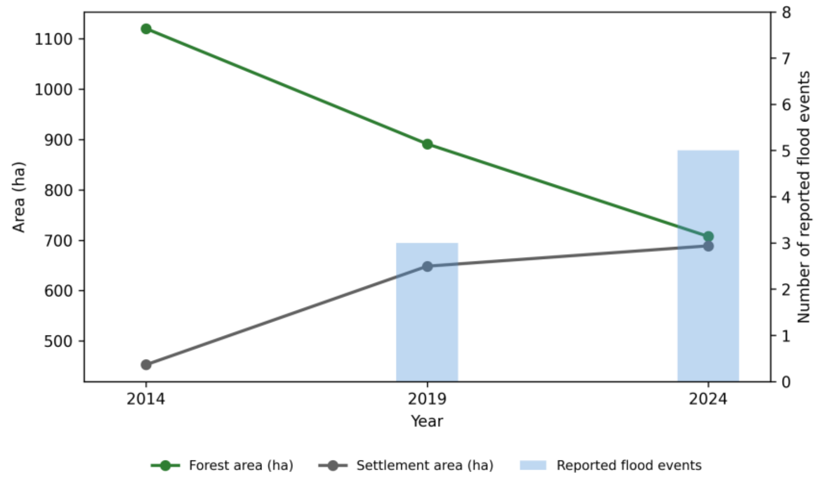

Figure 5. Temporal coincidence of land-cover changes and reported flood events

Two of the urban villages named in the available flood records, Sodohoa and Punggaloba, lie in the southern, low-lying part of West Kendari District, where Tables 5–7 show the largest gains in settlement and shrubland at the expense of forest and mixed garden, including forest and mixed-garden conversion to shrubland and settlement upslope of these villages between 2014 and 2024. This spatial co-location is consistent with, but does not confirm, a contribution of upstream land-cover changes to the flooding reported in these villages; a formal spatial overlay of geocoded flood points onto the transition maps was not possible with the flood records available for this study and is recommended as a direct next step.

It is important to separate what was directly measured from what is inferred. Directly measured in this study are the areas and transition pathways of six land-cover classes between 2014 and 2024 (Tables 3, 5–7) and the count of BPBD-reported flood events in 2014, 2019, and 2024. Observed as a pattern, rather than established with a formal statistical test, is the temporal coincidence between declining forest cover, expanding settlement and shrubland, and a rising count of reported flood events [35]. Inferred, and not established by this study, is a causal mechanism linking these two patterns. Alternative and confounding explanations that were not measured or controlled for in this study include year-to-year rainfall variability, obstruction or narrowing of drainage channels, the physical capacity of the district's rivers, channel sedimentation, local topography and soil infiltration characteristics, coastal tidal conditions, and changes in the population and number of buildings exposed to inundation over time. This last point matters because an increase in the number of reported flood events can also reflect improved disaster reporting and monitoring, or greater exposure from settlement expansion into flood-prone land, rather than solely a change in the physical processes that generate floods; in other words, the data available to this study cannot fully distinguish an increase in flood hazard from an increase in exposure or vulnerability. Given a comparison across only three time points and the absence of rainfall, drainage, and hydrological data, the independent contribution of land-cover change to the observed increase in reported flood occurrence cannot be statistically isolated in this study.

Comparison with Previous Studies

The pattern of forest and mixed-garden conversion into settlement and shrubland observed in West Kendari District is broadly consistent with land-cover change reported for other rapidly urbanizing Indonesian coastal cities, where peripheral agricultural and forested land is progressively converted to settlement as urban areas expand (Surya et al., 2021. It also parallels earlier flood-hazard assessments for Kendari City itself, which identified a large share of the city as exposed to flooding and linked this partly to reduced water-catchment capacity [36], [37]. The present study extends this earlier work by providing an area-reconciled, class-level account of land-cover change specifically for West Kendari District over a ten-year period. Unlike hydrological-modeling studies elsewhere, however, this study did not simulate runoff or infiltration directly, so it cannot confirm the magnitude of any runoff increase implied by the observed land-cover change, and this comparison with the literature should be read as contextual rather than confirmatory.

The conversion of shrubland into settlements indicates the development of new built-up areas, which interrupts natural vegetation succession. In contrast, settlements changed to shrubland in several abandoned locations, including parts of the community relocation area in Punggaloba Urban Village. Another prominent transition was the conversion of shrubland into mixed garden as local agricultural activity intensified. Along the coast, transitions among water bodies, mangroves, and settlements were influenced by land reclamation, sedimentation, and coastal abrasion [38], [39]. These interpretations, natural regeneration in the northern and eastern part of the district, reclamation and abrasion along the coast, and conversion driven by relocation or agricultural intensification, are consistent with the observed spectral change and with patterns documented for comparable Indonesian settings, but they were not independently confirmed in this study with field observation, high-resolution historical imagery, or local planning and permit records. They should therefore be treated as plausible explanations to be verified with such evidence in future work rather than as established fact.

Taken together, these patterns indicate a broader shift from vegetated land toward cultivated areas and settlements. This shift reduces water-catchment areas and expands impervious surfaces, potentially altering the district's hydrological characteristics. Land-cover change of this kind is generally expected, on hydrological grounds, to be associated with greater surface runoff and a reduced capacity for rainfall to infiltrate the soil; the present study did not measure runoff or infiltration directly and reports this as an expected mechanism rather than a measured outcome.

The effects of land-cover change may be reflected in the flooding experienced in West Kendari District. Several small rivers flow through the district, including the Watu-Watu, Tipulu, Lahundape, Lahundape Satu, Lahundape Dua, and Lasolo rivers, which together form a natural drainage system. As vegetation has declined, increased surface runoff is a plausible contributor to river channels and drainage infrastructure exceeding their capacity during high-intensity rainfall, although channel capacity and drainage condition were not directly measured in this study.

Study Limitations

- Only the 2024 land-cover classification was independently validated, using 26 reference points; the 2014 and 2019 classifications were not field-validated, so their accuracy is unknown and transition pathways involving these years should be treated as indicative.
- Twenty-six reference points across six classes is a small sample for a multi-class accuracy assessment, particularly for the water-body and mangrove classes, each represented by only one reference point; the reported class-level accuracies for these two classes should be treated as provisional, and expanded, well-distributed reference sampling per class is recommended.
- The Landsat scenes used for the three years could not be matched precisely for season, cloud cover, and tidal stage, which may introduce apparent change along the coastline that reflects imaging conditions rather than genuine land-cover conversion.
- The flood-event record spans only three observation years and relies on secondary BPBD reports without independently compiled rainfall, drainage, or river-capacity data; it cannot support a statistically controlled or spatially explicit relationship analysis, and part of the apparent increase in event counts may reflect improved reporting rather than solely a change in physical flood-generating processes.
- This study did not collect or analyze economic-loss data, and no economic-loss estimate is reported.
- The spatial analysis is limited to the administrative boundary of West Kendari District and does not explicitly incorporate upstream watershed contributions from outside the district.

Because of these limitations, this study is best characterized as a reconciled, descriptive account of land-cover change in West Kendari District that documents a temporal coincidence with reported flood occurrence, rather than as a validated causal or predictive analysis of flood risk.

These findings suggest, on a conditional and precautionary basis, that controlling further land conversion, protecting remaining forest and mangrove cover, improving drainage capacity, and pursuing sustainable spatial planning may be prudent components of a broader flood-mitigation strategy for West Kendari District, pending confirmation through the spatially explicit, rainfall-adjusted analysis recommended above; this study does not itself demonstrate that these measures would reduce flood risk by a specific amount.

CONCLUSION

Between 2014 and 2024, land cover in West Kendari District changed substantially. Based on the reconciled, area-consistent classification, forest cover declined from 1,119.92 ha (49.8%) in 2014 to 707.45 ha (31.5%) in 2024, a decrease of 412.47 ha (–36.8%). Over the same period, settlement area increased from 452.91 ha (20.1%) to 688.82

ha (30.6%), an increase of 235.91 ha (+52.1%), and shrubland expanded from 72.13 ha (3.2%) to 434.64 ha (19.3%), an increase of 362.51 ha (+502.6%). The dominant transition pathways were the conversion of forest into shrubland and mixed garden and the conversion of mixed garden into settlement. Independent accuracy assessment, available only for the 2024 classification, indicated an overall accuracy of 88.46% and a corrected Kappa coefficient of 0.851 (almost perfect agreement); because the 2014 and 2019 maps were not independently validated, this accuracy assessment should be understood to support the 2024 map specifically and should not be generalized to the earlier maps or to the full 2014–2024 series without further validation.

Reported flood events in West Kendari District, compiled from BPBD records, rose from none in 2014 to three in 2019 and five in 2024. Forest decline and settlement expansion coincided in time with this increase in reported flood events. However, the independent contribution of land-cover change to this increase could not be determined in this study, because rainfall variability, drainage capacity, river condition, sedimentation, coastal tides, and changes in population exposure were not quantitatively analyzed alongside land cover; the apparent increase in flood frequency may also partly reflect improved disaster reporting over time rather than a change in flood-generating processes alone. Economic losses associated with these floods were not quantified in this study.

These findings answer the study's two research questions: land cover in West Kendari District changed substantially toward built-up and shrubland classes between 2014 and 2024, and this change coincided in time with an increase in reported flood occurrence, without establishing a causal or statistically quantified relationship. A longer, spatially explicit, and rainfall-adjusted flood record; independent field validation of each classified year; and hydrological or statistical modeling that controls for confounding factors are recommended as the next steps toward a defensible assessment of the contribution of land-cover change to flood risk in West Kendari District.

ACKNOWLEDGMENTS
The authors thank the Master's Program in Environmental Management at Hasanuddin University's Graduate School for the academic support provided throughout this study. They also thank the Kendari City Government, the Kendari City Regional Disaster Management Agency (BPBD), and all other agencies and individuals who assisted with data provision, field surveys, and the information required for the research. The authors are also grateful to their academic supervisors and everyone who offered comments, suggestions, and corrections that helped bring this article to completion.

REFERENCES

[1] F. Nugraha, D. P. T. Baskoro, and S. D. Tarigan, “Evaluasi algoritma machine learning untuk klasifikasi dan prediksi penggunaan lahan,” *Maj. Geogr. Indones.*, vol. 39, no. 1, pp. 19–28, 2025, doi: 10.22146/mgi.99150.

[2] M. Arif, S. Sengupta, S. K. Mohinuddin, and K. Gupta, “Dynamics of land use and land cover change in peri-urban area of Burdwan City, India: a remote sensing and GIS-based approach,” *GeoJournal*, vol. 88, pp. 4189–4213, 2023.

[3] Ridwan, “Studi kajian dampak perubahan tutupan lahan terhadap kejadian banjir di daerah aliran sungai,” *ENVIRO J. Trop. Environ. Res.*, 2024.

[4] M. Kamaraj and S. Rangarajan, “Predicting the future land use and land cover changes for Bhavani basin, Tamil Nadu, India, using QGIS MOLUSCE plugin,” *Environ. Sci. Pollut. Res.*, vol. 29, pp. 86337–86348, 2022.

[5] P. Lukas, A. M. Melesse, and T. T. Kenea, “Prediction of future land use/land cover changes using a coupled CA-ANN model in the upper Omo-Gibe river basin, Ethiopia,” *Remote Sens.*, vol. 15, p. 1148, 2023.

[6] V. Nasiri, A. Deljouei, F. Moradi, S. M. M. Sadeghi, and S. A. Borz, “Land use and land cover mapping using Sentinel-2, Landsat-8 satellite images, and Google Earth Engine: a comparison of two composition methods,” *Remote Sens.*, vol. 14, no. 9, p. 1977, 2022.

[7] K. A. Hossain, M. Masiero, and F. Pirotti, “Land cover change across 45 years in the world’s largest mangrove forest (Sundarbans): the contribution of remote sensing in forest monitoring,” *Eur. J. Remote Sens.*, vol. 57, no. 1, 2024, doi: 10.1080/22797254.2022.2097450.

[8] O. A. Fashae, “Comparative assessment of the changing pattern of land cover along the Southwestern coast of Nigeria using GIS and remote sensing techniques,” *Sci. African*, vol. 17, no. 6, p. e01286, 2022.

[9] M. L. Edamo, “Capability of logistic regression in identifying flood-susceptible areas in a small watershed,” *H2Open J.*, vol. 7, no. 5, pp. 351–374, 2024.

[10] T. S. Miller, D. B. Wright, and S. Hassan, “Calibration of runoff curve numbers in highly modified tropical urban environments,” *Hydrol. Process.*, vol. 37, no. 2, p. e14780, 2023.

[11] M. N. Ahmad, Z. Shao, and A. Javed, “Mapping impervious surface area increase and urban pluvial flooding using Sentinel Application Platform (SNAP) and remote sensing data,” *Environ. Sci. Pollut. Res.*, vol. 30, no. 60, pp. 125741–125758, 2023, doi: 10.1007/s11356-023-30990-y.

[12] L. M. Prayoga, “Land cover classification assessment using decision trees and maximum likelihood classification algorithms on Landsat 8 data,” *DoubleClick J. Comput. Inf. Technol.*, vol. 6, no. 2, pp. 69–76, 2023,

doi: 10.25273/DOUBLECLICK.V6I2.10606.

[13] N. S. Ahmed and H. M. Abduljabbar, “Maximum likelihood classification for land cover change detection utilizing Landsat 8 imagery in Wasit Governorate,” *Ibn Al Haitham J. Pure Appl. Sci.*, vol. 36, no. 1, 2023.

[14] G. Mancino, A. Falciano, R. Console, and M. L. Trivigno, “Comparison between parametric and non-parametric supervised land cover classifications of Sentinel-2 MSI and Landsat-8 OLI data,” *Geographies*, vol. 3, no. 1, pp. 82–109, 2023, doi: 10.3390/geographies3010005.

[15] Y. Gurjar, R. Wen, E. Farahbakhsh, and R. Chandra, “Landcover classification and change detection using remote sensing and machine learning: a case study of Western Fiji,” 2025. doi: 10.48550/arXiv.2509.13388.

[16] Endarsih, “Model spasial perubahan penggunaan lahan dan tutupan lahan terhadap bencana banjir di Daerah Aliran Sungai Sikilang, Pasaman Barat,” *EL-JUGHRAFIYAH*, 2024.

[17] C. J. White, H. Carlsen, and A. W. Robertson, “Projecting localized extreme rainfall under accelerated climate change scenarios,” *Clim. Change*, vol. 178, no. 1, p. 12, 2025.

[18] R. Mulyasari, N. Haerudin, D. Rizkiani, and I. Akbari, “Pengaruh perubahan tutupan lahan terhadap pola banjir di Ibu Kota Provinsi Lampung: studi menggunakan SIG dan pendekatan temporal,” *OPHIOLITE J. Geol. Terap.*, vol. 6, no. 1, pp. 29–35, 2024, doi: 10.56099/ophi.v6i1.p29-35.

[19] C. M. Kaya and L. Derin, “Parameters and methods used in flood susceptibility mapping: a review,” *J. Water Clim. Chang.*, vol. 14, pp. 1935–1960, 2023.

[20] I. R. Khan, S. I. Elmahdy, R. Rustum, Q. Khan, and M. M. Mohamed, “Floods modelling and analysis for Dubai using HEC-HMS model and remote sensing using GIS,” *Sci. Rep.*, vol. 14, p. 25039, 2024.

[21] K. Ma, X. Li, Q. Liu, W. Zhou, and W. Li, “Application of SCS-CN method in flood hazard mapping,” *Front. Environ. Sci.*, vol. 13, p. 1713793, 2025.

[22] H. H. Nguyen, M. Venohr, A. Gericke, A. Sundermann, E. A. R. Welti, and P. Haase, “Dynamics in impervious urban and non-urban areas and their effects on run-off, nutrient emissions, and macroinvertebrate communities,” *Landsc. Urban Plan.*, vol. 231, p. 104639, 2023.

[23] A. M. Vincent, K. Parthasarathy, and P. Jidesh, “Flood susceptibility mapping using AutoML and a deep learning framework with evolutionary algorithms for hyperparameter optimization,” *Appl. Soft Comput.*, vol. 148, p. 110846, 2023.

[24] Z. Luo, J. Tian, J. Zeng, and F. Pilla, “Resilient landscape pattern for reducing coastal flood susceptibility,” *Sci. Total Environ.*, vol. 856, p. 159087, 2023.

[25] M. D. K. L. Gunathilaka and S. L. J. Fernando, “Accuracy assessment of unsupervised land use and land cover classification using remote sensing and geographical information systems,” *Int. J. Environ. Eng. Educ.*, vol. 4, no. 3, pp. 76–82, 2022.

[26] E. Allegri, M. Zanetti, S. Torresan, and A. Critto, “Pluvial flood risk assessment for 2021-2050 under climate change scenarios in the Metropolitan City of Venice,” *Sci. Total Environ.*, vol. 914, 2024.

[27] T. S. Onajomo, “Geospatial assessment of land use/cover, rainfall, and flood incidents in Eti-Osa, Lagos, Nigeria,” *South African J. Geomatics*, vol. 11, no. 2, pp. 202–218, 2022.

[28] H. Zhang, H. Jia, C. Li, and Q. Zhang, “Exploring the driving factors of urban flood at the catchment scale: a case study of multitype megacities in China,” *Ecol. Indic.*, vol. 166, p. 112513, 2024.

[29] A. Salvati, “Flood susceptibility mapping using support vector regression and hyper-parameter optimization,” *J. Flood Risk Manag.*, vol. 16, no. 4, p. e12920, 2023.

[30] J. Wang, M. Bretz, M. A. A. Dewan, and M. A. Delavar, “Machine learning in modelling land-use and land cover-change (LULCC): current status, challenges and prospects,” *Sci. Total Environ.*, vol. 822, p. 153559, 2022.

[31] M. Abdelkareem and A. M. Mansour, “Risk assessment and management of vulnerable areas to flash flood hazards in arid regions using remote sensing and GIS-based knowledge-driven techniques,” *Nat. Hazards*, vol. 117, no. 3, pp. 2269–2295, 2023.

[32] L. Ouyang *et al.*, “Mapping impervious surface using phenology-integrated and Fisher transformed linear spectral mixture analysis,” *Remote Sens.*, vol. 14, no. 7, p. 1673, 2022.

[33] K. L. Wong, Y. X. Chen, and H. S. Lim, “River buffer zone encroachment and channel capacity degradation in emerging Asian megacities,” *Land use policy*, vol. 137, p. 106981, 2024.

[34] T. E. Idowu, R. M. Waswa, K. Lasisi, M. Nyadawa, and V. Okumu, “Object-based land use/land cover change detection of a coastal city using multi-source imagery: a case study of Lagos, Nigeria,” *South African J. Geomatics*, vol. 9, pp. 136–148, 2022.

[35] M. S. Chowdhury, “Comparison of accuracy and reliability of random forest, support vector machine, artificial neural network and maximum likelihood method in land use/cover classification of urban setting,” *Environ. Challenges*, 2024.

[36] M. Banjara, A. Bhusal, A. B. Ghimire, and A. Kalra, “Impact of land use and land cover change on hydrological processes in urban watersheds: analysis and forecasting for flood risk management,” *Geosciences*, vol. 14, no. 2, p. 40, 2024, doi: 10.3390/geosciences14020040.

[37] R. Madhuri, K. Srinivasa Raju, and A. Vasan, “Flood-susceptibility-based building risk under climate change,

Hyderabad, India," *J. Water Clim. Chang.*, vol. 14, no. 7, pp. 2150–2163, 2023.

[38] O. O. Agumagu, R. Marchant, and L. C. Stringer, "Land use and land cover change dynamics in the Niger Delta region of Nigeria from 1986 to 2024," *Land*, vol. 14, no. 4, p. 765, 2025, doi: 10.3390/land14040765.

[39] B. Pradhan, "Spatial flood susceptibility mapping using an explainable artificial intelligence (XAI) model," *Geosci. Front.*, vol. 14, no. 6, p. 101625, 2023.